When $R > 0.8\ R_0$: Fluorescence Anisotropy, Non-additive Intensity, and Cluster Size

Z. Zolmajd-Haghighi*† and Q. S. Hanley*

*School of Science and Technology
Nottingham Trent University
Clifton Lane
Nottingham NG11 8NS
United Kingdom

†Current Address:
Institute of Biochemistry and Biophysics
University of Tehran,
Tehran
Iran

*** Corresponding author:** Q. S. Hanley

Methods and Applications of Fluorescence

Revised April/May 2016

Abstract:

Assembly and clustering feature in many biological processes and homo-FRET and fluorescence anisotropy can assist in estimating the aggregation state of a system. The distance dependence of resonance energy transfer is well described and tested. Similarly, assessment of cluster size using steady state anisotropy is well described for non-oriented systems when $R < 0.8\ R_0$, however, these methods break down when $R > 0.8\ R_0$. Fused trimeric DNA clusters labelled with fluorescein were engineered to provide inter-fluorophore distances from 0.7 to 1.6 R/R_0 and intensity and anisotropy were measured. These constructs cover a range where anisotropy effects depend on distance. Analytical expressions were derived for fully labelled and fractionally labelled clusters and the experimental results analysed. The experimental results showed that: 1) the system underwent distance dependent quenching; 2) when incompletely labelled both doubly and triply labelled forms could be assessed to obtain distance dependent intensity factors; 3) the anisotropy behaviour of a multiply labelled cluster of a particular size depends on the behaviour of the fluorophores and their distance in a cluster. This work establishes that when emission intensity data are available the analytically useful range for investigating clusters does not have to be restricted to $R < 0.8\ R_0$ and is applicable to cases where the anisotropy of a cluster of N fluorophores is not well approximated by r_1/N.

Introduction:

Many biological functions and malfunctions, involve self-assembly of proteins. Protein clustering has an important role in signal transduction through the cell membrane. Measurement of aggregation is a challenge particularly in cells and part of this challenge is properly accounting for the real behavior of typical fluorescence dyes upon clustering (1). Non-invasive analytical techniques such as methods based on Förster Resonance Energy Transfer (FRET) that probe protein self–assembly in their physiological context have been widely used to study protein aggregation (2).

A variety of approaches to measuring the size of a cluster using homo-FRET have been described using fluorescence anisotropy as an indicator of cluster size (1, 3, 4). These models of fluorescence anisotropy in clusters usually include the assumptions of equal fluorescence efficiency, random orientation, and the distance, R, is less than 0.8 of the Förster radius, R_o. With this set of assumptions, anisotropy gives an unambiguous relationship to cluster size and estimation of the anisotropy of the cluster is given conveniently by the anisotropy of the fluorophore in isolation, r_1, divided by the number of fluorophores in the cluster, N. However, many biological systems exceed this scale and, to meet the criteria, the FRET efficiency must be greater than 79%. In biological systems, this is rarely observed and when using FPs is nearly impossible to achieve. The values of homo-FRET Förster radii tabulated by Patterson *et al*. (2) suggest the largest distance allowed is 4.1 nm (for YFP). This is less than the 4.2 nm length of typical FPs (5) making 0.8 R_o possible only in a side on geometry. The 0.8R_o distances for the blue, cyan, green, and red variants are 2.09 nm, 2.62 nm, 3.72 nm, and 2.83 nm, respectively. For these variants, achieving 0.8 R_o ranges from impossible to challenging particularly when fused to a protein of interest. Further, as the distance approaches those requiring an ordered environment, the assumptions such as random orientation often applied may not hold. These considerations indicate that careful

investigation of the behaviour of systems in which $R > 0.8\ R_o$ and/or the anisotropy of a cluster with N fluorophores, r_N, is not equal to r_1/N is needed to better understand realistic behaviour in many biological systems.

Here we report an engineered set of DNA constructs containing up to three labels spanning the range from 0.7 to 1.6 R/R_o. These constructs provide an initial model in which the distances between the fluorophores are reasonably predictable giving a range of different sizes with a known and controllable number of fluorophores. With these materials, we could assess approaches to modelling the intensity and anisotropy of clustered materials while providing good control over distance.

Theory

The fluorescence anisotropy of a mixture is the intensity weighted sum over the individual anisotropies,

$$r(N) = \sum_{i=1}^{N} \phi_i r_i \qquad (1)$$

where ϕ_i and r_i are the fractional contribution to intensity and anisotropy of species i, respectively, and N is the number of labelled species in the mixture. Here, N will be assumed to be equivalent to the number of binding sites and i the number of labels for a given species.

The fluorescence intensity of a species with multiple fluorophores attached may exhibit a steady increase of intensity as the fractional labelling increases (6), however, more generally clusters of fluorophores in close proximity can also undergo self-quenching (1) or give enhanced emission (7). The fractional contribution for the general case is

$$\phi_i = \frac{z_i f_i}{\sum_{i=0}^{N} z_i f_i} \qquad (2)$$

where z_i is the relative intensity of a cluster of i fluorophores relative to the singly labelled form, and f_i is the fraction of the total having i labels attached.

If the mixture of fluorescently labelled species is the result of a stochastic mixture defined by the binomial distribution, the values of f_i may be computed from the maximum number of dyes in a cluster (N) and the average occupancy, $\bar{i}$ (4, 6):

$$f_i = \binom{N}{i}\left(\frac{\bar{i}}{N}\right)^i\left(1-\frac{\bar{i}}{N}\right)^{N-i} \qquad (3)$$

Using these equations, an expression for the anisotropy of a binomially defined mixture may be obtained (1, 4).

$$r(f,N) = \frac{\sum_{i=1}^{N} A_{i,N} z_i f^i (1-f)^{N-i} r_i}{\sum_{i=1}^{N} A_{i,N} z_i f^i (1-f)^{N-i}} \qquad (4)$$

In this expression, (A_1 , A_2 ,… A_N) are the coefficients from the (N-1) row of Pascal's triangle and f is the fraction of subunits labeled.

In clusters of fluorophores where $R < 0.8R_o$, the anisotropies r_1 to r_N are well approximated by r_1/N. However, this is a simplification of the distance dependent form which also includes the anisotropy of the molecule excited via energy transfer, r_{ET} (3):

$$r_N = r_1 \frac{1+(R_0/R)^6}{1+N(R_0/R)^6} + r_{ET} \frac{(N-1)(R_0/R)^6}{1+N(R_0/R)^6} \quad (5)$$

This expression indicates the anisotropy of multiply labeled species can be divided into 3 zones (Figure 1): i) when $R < 0.8\ R_o$, the anisotropy is approximately independent of distance and $r_N \approx r_1 / N$; ii) when $0.8\ R_o < R < 2.2\ R_o$, the anisotropy of the species is strongly dependent on distance and anisotropy alone gives an ambiguous indication of the number of fluorophores in a cluster; iii) at larger values of R, $r_N \approx r_1$ for the smaller clusters.

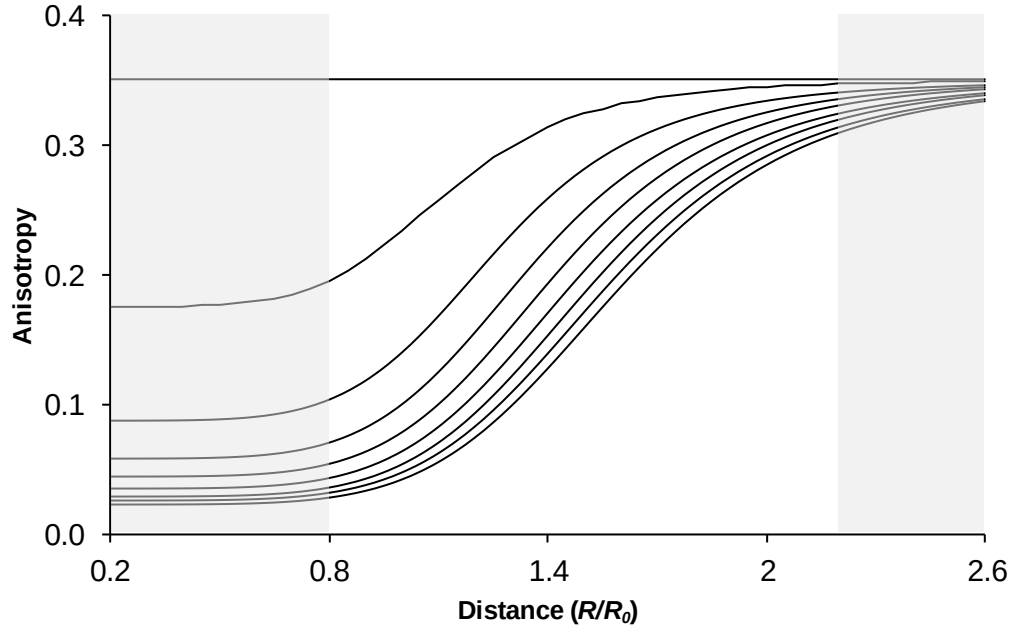

Figure 1: Simulation of the distance dependence of anisotropy as cluster size increases. The shaded zone on the right indicates the behaviour of clusters when $R < 0.8\ R_o$,. The middle region is when $0.8\ R_o < R < 2.2\ R_o$. The left shaded region is when $R > 2.2\ R_o$. The uppermost line corresponds to an unclustered species with a single fluorophore with $r_1 = 0.35$ and $r_{ET} = 0.0$. The curves correspond to $N = \{2, 4, 6, 8, 10, 12, 14, 16\}$ going down the figure. It should be noted that the cut offs at 0.8 and 2.2 R_o are somewhat arbitrary.

Implicit in this model are the assumptions that energy transfer is fully reversible, the fluorophores are equivalent, and the product of the fluorescence lifetime and rate of energy transfer is $(R_0/R)^6$. The last of these only applies when the orientation factor, $\kappa^2 = 2/3$. This

case corresponds to dynamic randomization and is unlikely to apply to the semi-rigid DNA system in frozen solution investigated here. More detailed treatments are available (8), however, a factor, β_N, can be introduced into equation 5 which provides an indication of the extent to which the assumptions of the model are met.

$$r_N = r_1 \frac{1+\beta_N (R_0/R)^6}{1+N\beta_N (R_0/R)^6} + r_{RET} \frac{(N-1)\beta_N (R_0/R)^6}{1+N\beta_N (R_0/R)^6} \quad (6)$$

To a first approximation, β values are a surrogate for κ^2. However, in systems with a distance dependent partial reversibility or a distribution of distances, β will report on these process as well. When $\beta = 1$, the system follows the simplified model of equation 5.

Using this set of equations allows the distance dependent behaviour of engineered clusters of fluorophores at variable distances to be evaluated either as isolated clusters or in stochastic mixtures. These expressions require information about the values of z_i over a range of distances which must be assessed.

One approach to assessing values of z_i is to perform a titration (1) as the fractional labelling changes. In a system where labelling proceeds according to the binomial distribution, the normalised intensities can be fit.

$$I(f,N) = \sum_{i=1}^{N} A_{i,Ni} z_i f^i (1-f)^{N-i} \quad (7)$$

In practice, it is often useful to use the raw intensity values as an appropriate normalization factor is not always obvious.

$$I_M(f,N) = C\sum_{i=1}^{N} A_{i,Ni} z_i f^i (1-f)^{N-i} \quad (8)$$

Here, the values of I_M are raw measured intensities and C is a constant representing the intensity of the singly labelled species under the conditions of study. For a system with three sites, only 3 parameters are required: C, z_2, and z_3. The value of z_1 is always 1 as this is the relative intensity of the single fluorophore by itself.

When encountering a system of unknown characteristics, a range of complementary distance dependent phenomena may be used to obtain the clustering of a system. Here, we applied equation 8 to obtain distance dependent z_i values. This information allowed a set of distance dependent r_i values to be recovered and compared to theory. Although we used intensity data, a complementary distance dependent parameter like lifetime could also be used.

Materials and Methods

Fluorescence Measurements: Samples were measured in a fluorimeter fitted with polarisers (Tecan Infinite Pro 2000). Blank offset (9) and G-factor corrections were applied. Concentrations were kept ≥ 1μM to prevent artefacts. All measurements were done at the same gain setting with excitation at 485 nm with the bandwidth of 20 nm. Fluorescence emission was monitored at 535 nm with a 25 nm bandwidth. Verification that anisotropy changes were from homo-FRET was done by fractional labelling experiments and observation in frozen solutions (observed immediately after removal from -20ºC).

DNA Oligonucleotides: Oligonucleotides were obtained commercially (*Life Technologies, Paisley, UK*) and provided in concentrated form. The oligonucleotides were dissolved in a buffer solution of 10 mM Trizma hydrochloride, 1 mM EDTA and 50mM NaCl. The buffer components were dissolved in water and the pH adjusted to 7.5 with sodium hydroxide. Stock solutions (100 μM) of all oligonucleotides were prepared in this buffer. The oligonucleotides consisted of: a trimeric complement construct ranging in length from 41-65 bases with 0-12

base gaps between segments allowing hybridisation to a 9 base complement (GTGAGTCGT) labelled with 5' fluorescein. The templates for assembling the trimeric complements were: 41-mer: CCCCTAGCACTCAGCACACTCAGCACACTCAGCAGAAGGGG; 43-mer: CCCCTAGCACTCAGCAGCACTCAGCAGCACTCAGCAGAAGGGG; 45-mer: CCCCTAGCACTCAGCAGGCACTCAGCAGGCACTCAGCAGAAGGGG; 47-mer: CCCCTAGCACTCAGCACTGCACTCAGCACTGCACTCAGCAGAAGGGG; 49-mer: CCCCTAGCACTCAGCATCTGCACTCAGCATCTGCACTCAGCAGAAGGGG; 51-mer: CCCCTAGCACTCAGCATGAGGCACTCAGCATGAGGCACTCAGCAGAAGGGG; 53-mer CCCCTAGCACTCAGCATGCAGGCACTCAGCATGCAGGCACTCAGCAGAAGGGG; 55-mer: CCCCTAGCACTCAGCACTGCAGGCACTCAGCACTGCAGG CACTCAGCAGAAGGGG; 57-mer: CCCCTAGCACTCAGCACTGCAGGACAC TCAGCACTTGCAGACACTCAGCAGAAGGGG; 61-mer: CCCCTAGCACTCA GCACTCTGCAGGACACTCAGCACTCTTGCAGACACTCAGCAGAAGGGG; 65-mer: CCCCTAGCACTCAGCACTCTCTGCAGGACACTCAGCACTCTCTTG CAGACACTCAGCAGAAGGGG.

Fractional labelling of DNA strands: The trimeric complement systems were fractionally labelled by varying the amount of available fluorescently labelled complement such that the upper limit of the range was sufficient to allow saturation of the template DNA. All templates were titrated over a molar ratio from 0.05:1 up to 3:1. The complementary sequence concentration was kept above 1 μM to provide robust anisotropy measurements.

Results and Discussion

Intensity and Quenching

To assess how systems behave when $R > 0.8\ R_0$, the trimeric DNA templates were titrated with the labelled complementary sequence (Figure 2). Models based on binomially distributed species with varying z_i values (1) were fit to each construct following equation 8 (example, Figure 3). If the assumption of equal fluorescence efficiency (6, 10) applied, a straight line would be expected. This was not observed and there was good correspondence to the binomial model with quenching (equation 8). The constructs showed nearly ideal behaviour and almost the same increase of intensity up to $f \approx 0.2$ (Figure 2). Beyond this they began to exhibit quenching. The constructs became brighter as the distance increased and the shortest template showed the greatest amount of quenching (~50%). None exhibited equal fluorescence efficiency (Figure 2, solid line) with all showing some degree of quenching in both doubly and triply labelled forms. This behaviour is consistent with the known behaviour of most dyes which show quenching or enhancing behaviour in close proximity (7, 11-21). Fluorescein in particular shows strong quenching (22), however, the distance dependence of this quenching has not been reported in detail.

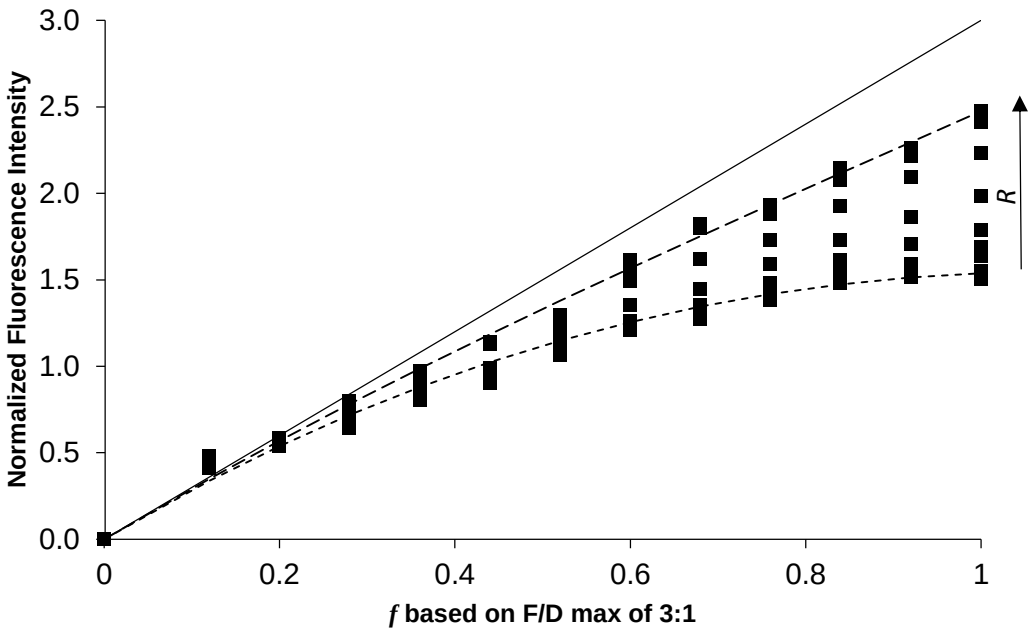

Figure 2: Titration of 11 trimeric DNA templates with fluorescein labelled complement. The samples had estimated distances between neighbouring dyes, R_{12}, from ≈ 31 Å (lower short dashed line) to ≈ 71 Å (long dashed line). However the intensities obtained from the shorter

DNA templates were remarkably lower. The solid line shows theoretical intensities, calculated based on the assumption of equal fluorescence efficiency. In the figure, F/D is the maximum fluorophore to DNA construct ratio and *f* is the fractional occupancy.

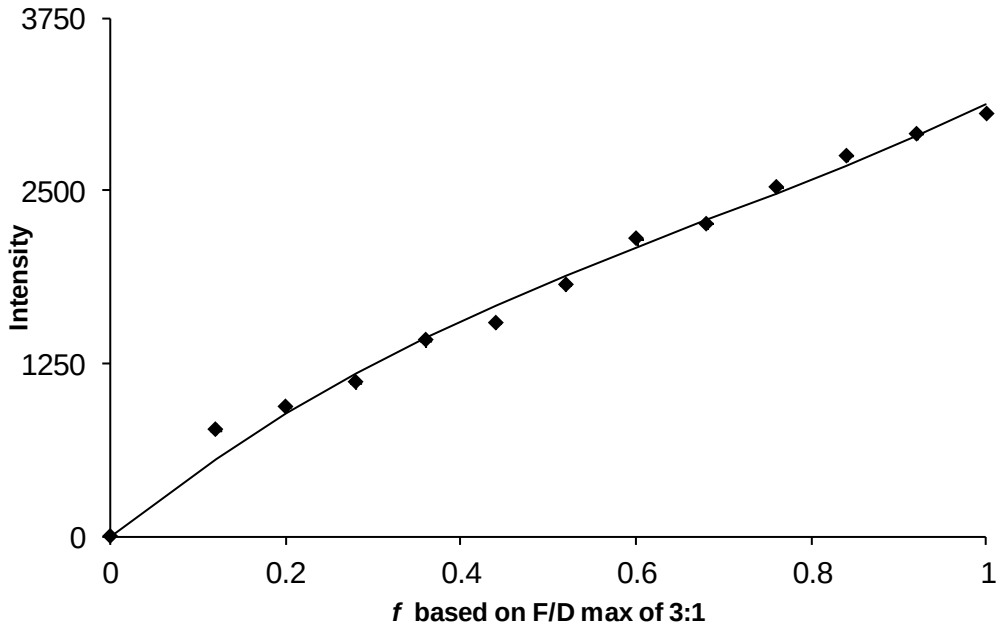

Figure 3: Fit of the fractional labelling curve to obtain values of C, z_2, and z_3. Data shown is for the construct of length 51 bp in which fluorophores are separated by 14 bases. The value of z_1 was set to 1 and the parameters obtained from the fit were C = 1710, z_2 = 1.25 and z_3 = 1.82. Ideal z_i values would be {1, 2, 3} in the absence of quenching.

The framework for assessing quenching (1) using equation 8 assumes each solution to be a stochastic mixture of differently labelled DNA. In trimeric DNA systems, such addition is not always observed (23), however, here the binomial model fit well giving a set of z_i values that varied with distance (Figure 4). Two points are notable in this data. First, it makes clear that energy migration via homo-FRET is an important aspect of quenching in clustered fluorophores. This distance dependent quenching will also affect the lifetime of the species involved. Consequently, distance can be assessed with a homo-FRET system undergoing quenching (Figure 5) and this should be added to the set of methods used to assess energy transfer. Second, there is a marked periodicity in the z_i values (Figure 4). This behaviour is likely similar to that reported in hetero-FRET assessment of DNA handedness (24). In that

study the distance between a FRET pair was varied giving a periodicity associated with the helical structure of DNA. Double stranded DNA of length 9 is nearly a complete turn of the helix with a second completed in a 21 base pair construct. However, most of the templates are incompletely hybridized due to the gaps between complementary sequences for the label. These will have an impact on the helix and the distances involved making them less predictable, however, there is clear periodicity with perhaps some evidence for orientation effects. The shortest distance is expected for a separation of 9 base pairs but the maximum quenching is closer to 13.

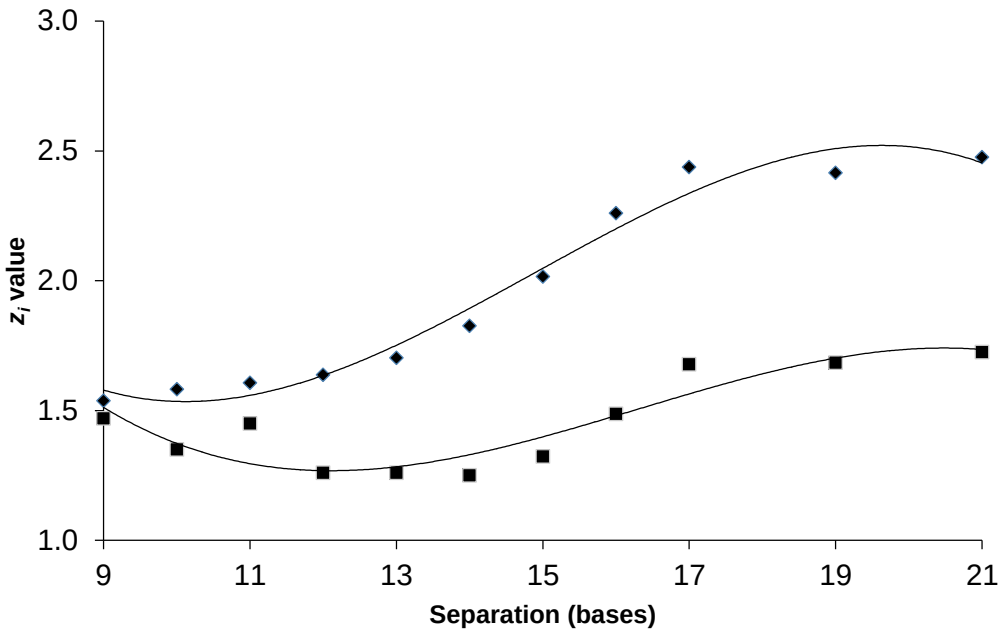

Figure 4: Comparison of the values of the fitted parameters z_2 (■) and z_3 (♦), for samples with different distances between dyes and consequently different extent of self-quenching. The z_2 and z_3, factors showed an increase with distance, but z_2 and z_3 did not reach the theoretical values of 2 and 3, respectively. The solid lines are to guide the eye.

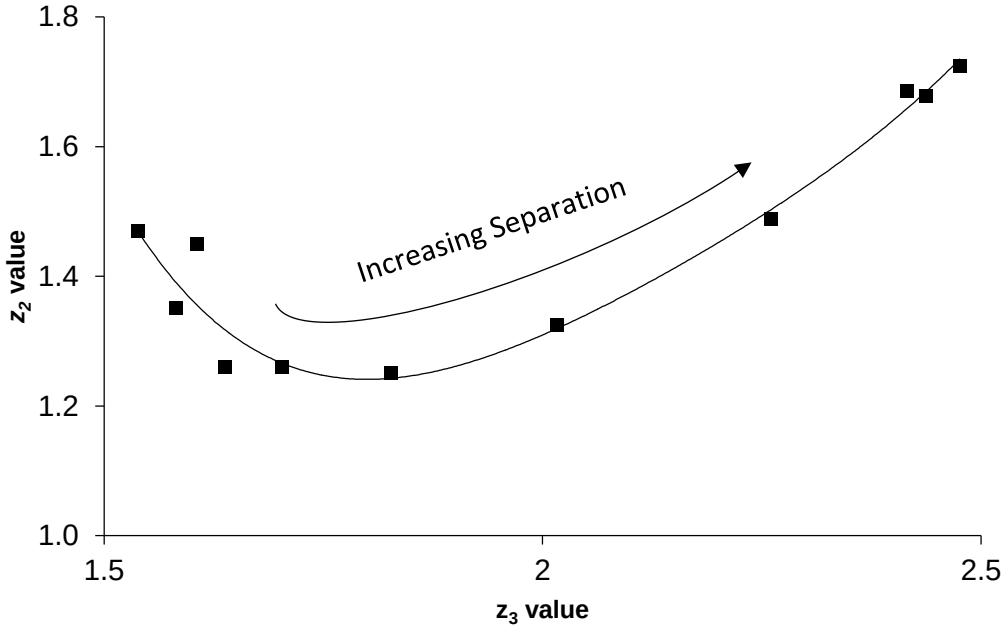

Figure 5: Relationship between z_2 and z_3, as the separation increased between fluorophores. The trajectory can be calibrated for the number of base pairs between fluorophores. Solid lines are to guide the eye.

Anisotropy

The trends in anisotropy were observed as fractional labelling was adjusted (Figure 6). Using the z_i factors (Figure 4) and equation 4, the anisotropies r_1, r_2 and r_3 were fit assuming r_{ET} was 0. A single r_1 was fit globally as this was expected to remain nearly constant. It is of interest that these titrations gave access to the doubly labelled species in this trimeric system, despite it never being present independent of the others allowing access to both z_2 and r_2. The resulting values of r_2 and r_3 were fit to equation 6 using R_0 = 4.4 nm (Figure 7). This gave β_2 = 0.22±0.03 and β_3 = 0.67±0.06 consistent with an orientation effect that is strongest in the doubly labelled species. This is believed due to a greater range of orientations available to a fluorophore is the species having three fluorophores. The value of R_0 used here is at the low end of the range reported in the literature for fluorescein (3, 19, 25-28); however, it provides a best case for the extent to which standard models fit this system. For larger assumed values of R_0, the deviations become more extreme in the direction of greater perpendicularity.

The values from the doubly labelled species exhibited more scatter and less correspondence to the expected trend than for the trimeric assembly. This is believed to be primarily due to r_2 never being observed directly, but may also arise from two doubly labelled species, 66% with the distance of R_{12} (or R_{23}) between the fluorophores and 33% with the distance of R_{13} (Scheme 1).

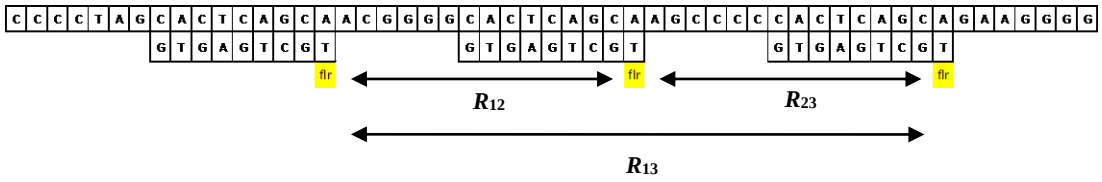

Scheme 1: An example of a DNA trimeric assembly with a gap of 6 nucleotides between the repeating sequences. R_{12} and R_{23} show the distances between two neighbouring dyes and are equal while R_{13} is greater.

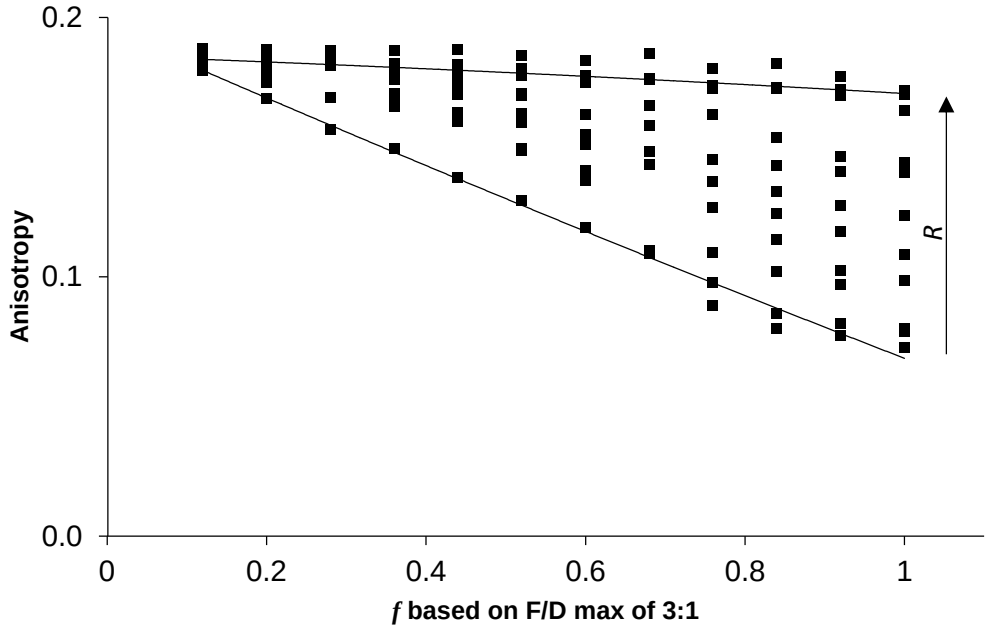

Figure 6: Comparison of anisotropies of the set of 11 different samples while the fractional labelling was adjusted by titrating with the labelled complementary sequence. The trends for the longest (upper solid line) and shortest (lower solid line) have been highlighted. All the measurements were done on samples that were frozen (-20°C) prior to measurement.

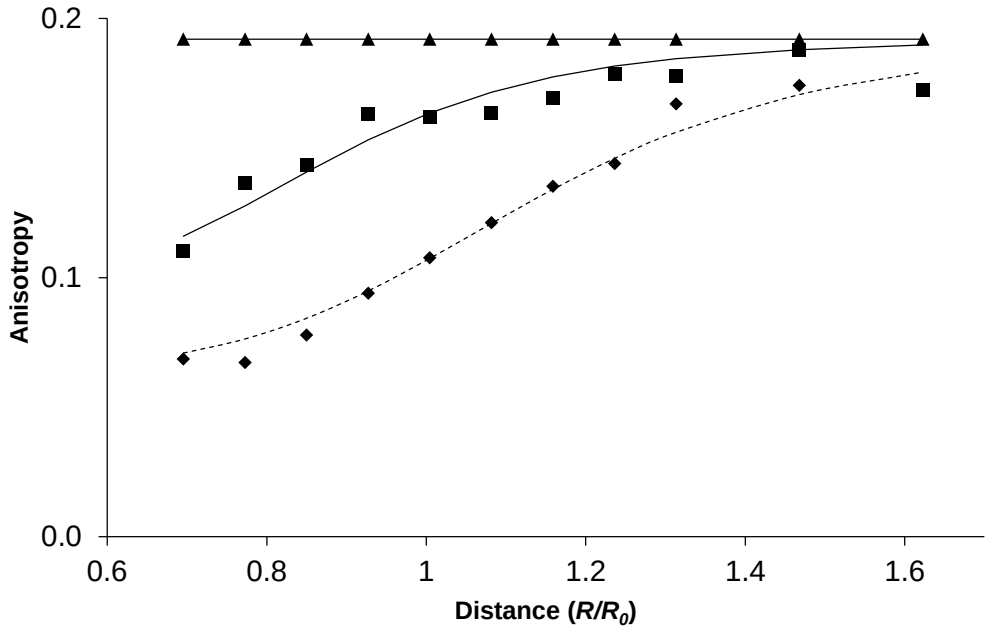

Figure 7: Comparison of 3 fitted parameters of data analysis: r_1, r_2, r_3 that show the anisotropies of different constructs with different numbers of labels: one label, r_1, (▲), two labels, r_2, (■) and three labels, r_3, (◆). The curves for r_2 and r_3 correspond to best fits to equation 6 with R_0 = 4.4 nm.

The analysis presented here relies on the assumption that the fractionally labelled species are defined by the binomial distribution. DNA is typically assumed to have linear structures (29), however, these were designed to have sticky ends allowing for circular forms. This gives some uncertainty to the exact distances involved and may also be responsible for the observed reduction in anisotropy in the larger templates. Using these constructs the general behaviour predicted by Runnels and Scarlatta is observed and, following further refinements to correct for the effects represented by β, good correspondence with theory is seen (Figure 7) when Equation 6 was used to estimate homo-FRET distance in a cluster with N = 3.

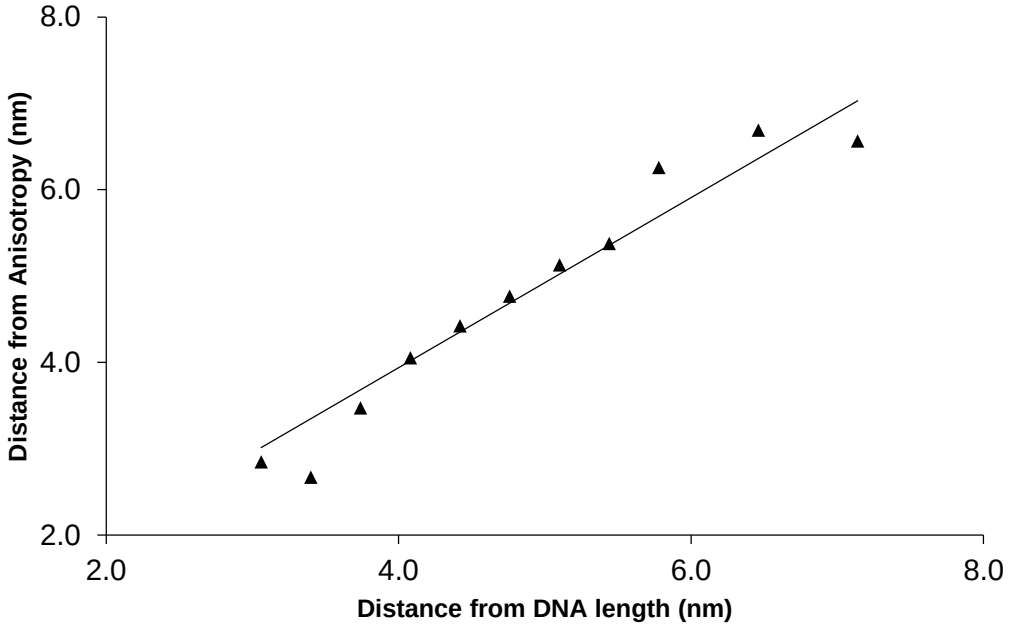

Figure 7: Comparison of distance based on DNA base length and distance obtained by fits to Equation 6. The anisotropy homo-FRET distances were on average ~2% lower than those estimated from the DNA base length.

Conclusion

Fluorescence anisotropy is widely applied to study aggregate formation in living cells (30). There are a number of well accepted theories (3, 4, 10, 31) to quantify cluster sizes. Here we have extended the reach of cluster assessment by showing that complementary information from intensity and steady state anisotropy may be used to recover distance dependent z_i and r_i values for mixed clusters. The emission intensity of individual species helps us to estimate r_N in a stochastic mixture when $r_N \neq r_1/N$. This in turn makes the investigation of clusters above 0.8 R_0 a more tractable problem. The semi-rigid system investigated here is a more difficult case than would apply in solution due to orientation effects, however the approach shown here could be applied more generally. In these cases, the problematic range could extend well below 0.8 R_0 due to orientation effects causing deviations from standard assumptions.

The theory presented here can use the information obtained from intensity data to understand measured anisotropy in multiply labelled systems containing mixed species. By knowing the intensity of differently labelled species in a stochastic mixture, the distance can be estimated and used to compute FRET efficiency and inform interpretation of the fluorescence anisotropy. This in turn makes feasible the assessment of cluster size over a more realistic range ($R/R_o > 0.8$) for biological systems. We anticipate combining intensity imaging and complementary methods with steady state anisotropy will be of great value when adapted for work *in vivo* (32-36). Additional detailed investigations of similar systems using lifetimes and dynamic anisotropy will be of great value particularly for understanding orientation effects and working with mixtures that do not follow the binomial distribution.

Author Contributions:

Designed research, analysed data, and wrote paper: Z. Zolmajd-Haghighi and Q. S. Hanley. Performed experiments: Z. Zolmajd-Haghighi.

Acknowledgements

The authors acknowledge funding from NanoSci-E+ to the NanoActuate consortium. In the UK, NanoActuate was administered by EPSRC as EP/H00694X/1. They also thank Prof. Carole Perry for use of the Tecan 200 Pro.

References

1. Zolmajd-Haghighi, Z., and Q. Hanley. 2014. When One Plus One Does Not Equal Two: Fluorescence Anisotropy in Aggregates and Multiply Labeled Proteins. Biophysical Journal 106:1457-1466.
2. Patterson, G. H., D. W. Piston, and B. G. Barisas. 2000. Förster distances between green fluorescent protein pairs. Analytical biochemistry 284:438-440.
3. Runnels, L. W., and S. F. Scarlata. 1995. Theory and application of fluorescence homotransfer to melittin oligomerization. Biophysical Journal 69:1569-1583.

4. Yeow, E. K. L., and A. H. A. Clayton. 2007. Enumeration of oligomerization states of membrane proteins in living cells by homo-FRET spectroscopy and microscopy: theory and application. Biophysical journal 92:3098-3104.
5. Ormö, M., A. B. Cubitt, K. Kallio, L. A. Gross, R. Y. Tsien, and S. J. Remington. 1996. Crystal structure of the Aequorea victoria green fluorescent protein. Science 273:1392-1395.
6. Weber, G., and E. Daniel. 1966. Cooperative Effects in Binding by Bovine Serum Albumin. II. The Binding of 1-Anilino-8-naphthalenesulfonate. Polarization of the Ligand Fluorescence and Quenching of the Protein Fluorescence. Biochemistry 5:1900-1907.
7. Cuppoletti, A., Y. Cho, J.-S. Park, C. Strässler, and E. T. Kool. 2005. Oligomeric fluorescent labels for DNA. Bioconjug. Chem. 16:528-534.
8. Berberan-Santos, M. N., P. Choppinet, A. Fedorov, L. Jullien, and B. Valeur. 1999. Multichromophoric cyclodextrins. 6. Investigation of excitation energy hopping by Monte-Carlo simulations and time-resolved fluorescence anisotropy. Journal of the American Chemical Society 121:2526-2533.
9. Ameloot, M., M. vandeVen, A. U. Acuña, and B. Valeur. 2013. Fluorescence anisotropy measurements in solution: Methods and reference materials (IUPAC Technical Report). Pure and Applied Chemistry 85:589-608.
10. Daniel, E., and G. Weber. 1966. Cooperative Effects in Binding by Bovine Serum Albumin. I. The Binding of 1-Anilino-8-naphthalenesulfonate. Fluorimetric Titrations*. Biochemistry 5:1893-1900.
11. Panchuk-Voloshina, N., R. P. Haugland, J. Bishop-Stewart, M. K. Bhalgat, P. J. Millard, F. Mao, W.-Y. Leung, and R. P. Haugland. 1999. Alexa dyes, a series of new fluorescent dyes that yield exceptionally bright, photostable conjugates. Journal of Histochemistry & Cytochemistry 47:1179-1188.
12. Voss Jr, E. W., C. Workman, and M. Mummert. 1996. Detection of protease activity using a fluorescence-enhancement globular substrate. BioTechniques 20:286-291.
13. Gruber, H. J., C. D. Hahn, G. Kada, C. K. Riener, G. S. Harms, W. Ahrer, T. G. Dax, and H. G. Knaus. 2000. Anomalous fluorescence enhancement of Cy3 and cy3.5 versus anomalous fluorescence loss of Cy5 and Cy7 upon covalent linking to IgG and noncovalent binding to avidin. Bioconjug. Chem. 11:696-704.
14. Anderson, G. P., and N. L. Nerurkar. 2002. Improved fluoroimmunoassays using the dye Alexa Fluor 647 with the RAPTOR, a fiber optic biosensor. Journal of immunological methods 271:17-24.
15. Kashida, H., K. Sekiguchi, X. Liang, and H. Asanuma. 2010. Accumulation of Fluorophores into DNA Duplexes To Mimic the Properties of Quantum Dots. Journal of the American Chemical Society 132:6223-6230.
16. Teo, Y. N., and E. T. Kool. 2012. DNA-multichromophore systems. Chemical Reviews 112:4221-4245.
17. Nguyen, T. A., P. Sarkar, J. V. Veetil, S. V. Koushik, and S. S. Vogel. 2012. Fluorescence polarization and fluctuation analysis monitors subunit proximity, stoichiometry, and protein complex hydrodynamics. PLoS ONE 7:e38209.
18. Gholami, Z., L. Brunsveld, and Q. Hanley. 2013. PNA-Induced assembly of fluorescent proteins using DNA as a framework. Bioconjug. Chem. in press.
19. Hungerford, G., J. Benesch, J. F. Mano, and R. L. Reis. 2007. Effect of the labelling ratio on the photophysics of fluorescein isothiocyanate (FITC) conjugated to bovine serum albumin. Photochem. Photobiol. Sci. 6:152-158.
20. Matveeva, E. G., E. A. Terpetschnig, M. Stevens, L. Patsenker, O. S. Kolosova, Z. Gryczynski, and I. Gryczynski. 2009. Near-infrared squaraine dyes for fluorescence enhanced surface assay. Dyes and Pigments 80:41-46.

21. Brinkley, M. 1992. A Brief Survey of Methods for Preparing Protein Conjugates with Dyes, Haptens, and Cross-Linking Agents. Bioconjug. Chem. 3:2-13.
22. Lakowicz, J. R. 2009. Principles of Fluorescence Spectroscopy. Springer.
23. Gholami, Z., and Q. Hanley. 2014. Controlled Assembly of SNAP–PNA–Fluorophore Systems on DNA Templates To Produce Fluorescence Resonance Energy Transfer. Bioconjug. Chem. 25:1820-1828.
24. Jares-Erijman, E. A., and T. M. Jovin. 1996. Determination of DNA helical handedness by fluorescence resonance energy transfer. J. Mol. Biol. 257:597-617.
25. Krishnan, R., R. Varma, and S. Mayor. 2001. Fluorescence methods to probe nanometer-scale organization of molecules in living cell membranes. Journal of Fluorescence 11:211-226.
26. Kawski, A. 1983. Excitation energy transfer and its manifestation in isotropic media. Photochemistry and photobiology 38:487-508.
27. Miller, J. N. 2005. Fluorescence energy transfer methods in bioanalysis. Analyst 130:265-270.
28. Chen, R. F., and J. R. Knutson. 1988. Mechanism of fluorescence concentration quenching of carboxyfluorescein in liposomes: energy transfer to nonfluorescent dimers. Analytical biochemistry 172:61-77.
29. Hogan, M., J. Wang, R. Austin, C. Monitto, and S. Hershkowitz. 1982. Molecular motion of DNA as measured by triplet anisotropy decay. Proceedings of the National Academy of Sciences 79:3518-3522.
30. Schierle, G. S. K., M. Sauer, and C. F. Kaminski. 2014. Probing Amyloid Aggregation and Morphology In Situ by Multiparameter Imaging and Super-Resolution Fluorescence Microscopy.
31. Knox, R. S. 1968. Theory of Polarization Quenching by Excitation Transfer. Physica 39:361-386.
32. Clayton, A. H. A., Q. S. Hanley, D. J. Arndt-Jovin, V. Subramaniam, and T. M. Jovin. 2002. Dynamic fluorescence anisotropy imaging microscopy in the frequency domain (rFLIM). Biophysical Journal 83:1631-1649.
33. Zhou, Y., J. M. Dickenson, and Q. S. Hanley. 2009. Imaging lifetime and anisotropy spectra in the frequency domain. Journal of microscopy 234:80-88.
34. van Ham, T. J., A. Esposito, J. R. Kumita, S.-T. D. Hsu, G. S. Kaminski Schierle, C. F. Kaminski, C. M. Dobson, E. A. Nollen, and C. W. Bertoncini. 2010. Towards multiparametric fluorescent imaging of amyloid formation: Studies of a YFP model of α-synuclein aggregation. J. Mol. Biol. 395:627-642.
35. Esposito, A., A. N. Bader, S. C. Schlachter, D. J. van den Heuvel, G. K. Schierle, A. R. Venkitaraman, C. F. Kaminski, and H. C. Gerritsen. 2011. Design and application of a confocal microscope for spectrally resolved anisotropy imaging. Opt Express 19:2546-2555.
36. Brasselet, S., P. Ferrand, A. Kress, X. Wang, H. Ranchon, and A. Gasecka. 2013. Imaging Molecular Order in Cell Membranes by Polarization-Resolved Fluorescence Microscopy. In Fluorescent Methods to Study Biological Membranes. Springer. 311-337.